

## RESEARCH ARTICLE

# Oxidative stress mediates nucleocytoplasmic shuttling of KPNA2 via AKT1-CDK1 axis-regulated S62 phosphorylation

Jie-Xin Huang<sup>1</sup>  | Chun-I Wang<sup>2</sup>  | Chia-Yu Kuo<sup>3</sup> | Ting-Wei Chang<sup>4</sup>  |  
Yu-Chin Liu<sup>3</sup>  | Ting-Feng Hsiao<sup>1,5</sup>  | Chih-Liang Wang<sup>6,7</sup>  | Chia-Jung Yu<sup>1,3,5,7</sup> 

<sup>1</sup>Graduate Institute of Biomedical Sciences, College of Medicine, Chang Gung University, Taoyuan, Taiwan

<sup>2</sup>Department of Biochemistry, School of Medicine, China Medical University, Taichung, Taiwan

<sup>3</sup>Department of Cell and Molecular Biology, College of Medicine, Chang Gung University, Taoyuan, Taiwan

<sup>4</sup>Institute of Molecular Medicine, College of Medicine, National Taiwan University, Taipei, Taiwan

<sup>5</sup>Molecular Medicine Research Center, Chang Gung University, Taoyuan, Taiwan

<sup>6</sup>School of Medicine, College of Medicine, Chang Gung University, Taoyuan, Taiwan

<sup>7</sup>Department of Thoracic Medicine, Chang Gung Memorial Hospital, Taoyuan, Taiwan

## Correspondence

Chia-Jung Yu, Department of Cell and Molecular Biology, College of Medicine, Chang Gung University, 259 Wen-Hwa 1st Road, Guishan District, Taoyuan, Taiwan.

Email: [yucj1124@mail.cgu.edu.tw](mailto:yucj1124@mail.cgu.edu.tw)

## Abstract

Karyopherin  $\alpha$  2 (KPNA2, importin  $\alpha$ 1), a transport factor shuttling between the nuclear and cytoplasmic compartments, is involved in the nuclear import of proteins and participates in cellular processes such as cell cycle regulation, apoptosis, and transcriptional regulation. However, it is still unclear which signaling regulates the nucleocytoplasmic distribution of KPNA2 in response to cellular stress. In this study, we report that oxidative stress increases nuclear retention of KPNA2 through alpha serine/threonine-protein kinase (AKT1)-mediated reduction of serine 62 (S62) phosphorylation. We first found that AKT1 activation was required for H<sub>2</sub>O<sub>2</sub>-induced nuclear accumulation of KPNA2. Immunoprecipitation and quantitative proteomic analysis revealed that the phosphorylation of KPNA2 at S62 was decreased under H<sub>2</sub>O<sub>2</sub>-induced oxidative stress. We showed that cyclin-dependent kinase 1 (CDK1), a kinase responsible for KPNA2 S62 phosphorylation, contributes to the localization of KPNA2 in the cytoplasm. AKT1 knock-down increased KPNA2 S62 phosphorylation and inhibited CDK1 activation. Furthermore, H<sub>2</sub>O<sub>2</sub>-induced AKT1 activation promoted nuclear KPNA2 interaction with nucleophosmin 1 (NPM1), resulting in attenuation of NPM1-mediated cyclin D1 gene transcription. Thus, we infer that the AKT1-CDK1 axis regulates the nucleocytoplasmic shuttling and function of KPNA2 through spatiotemporal regulation of KPNA2 S62 phosphorylation under oxidative stress conditions.

## KEYWORDS

KPNA2, NPM1, nucleocytoplasmic, oxidative stress, phosphorylation, proteomics

**Abbreviations:** AKT1, alpha serine/threonine-protein kinase 1; AMPK, AMP-activated protein kinase; ATM, Ataxia-telangiectasia mutated kinase; CCND1, cyclin D1; CDK1, cyclin-dependent kinase 1; DTT, dithiothreitol; FBS, fetal bovine serum; H<sub>2</sub>O<sub>2</sub>, hydrogen peroxide; IFA, immunofluorescence assay; IP, immunoprecipitation; KPNA2, karyopherin  $\alpha$ 2; LC-MS/MS, liquid chromatography–tandem mass spectrometry; m/z, mass-to-charge ratio; mTOR, the mammalian target of rapamycin; NPM1, nucleophosmin 1; PLA, proximity ligation assay; SILAC, stable isotope labeling by amino acids in cell culture; WEE1Hu, Wee1-like protein kinase; WT, wild-type.

This is an open access article under the terms of the [Creative Commons Attribution-NonCommercial](https://creativecommons.org/licenses/by-nc/4.0/) License, which permits use, distribution and reproduction in any medium, provided the original work is properly cited and is not used for commercial purposes.

©2024 The Author(s) *FASEB BioAdvances* published by The Federation of American Societies for Experimental Biology.

## 1 | INTRODUCTION

Nucleocytoplasmic transport is critical for cell physiology and various cellular processes. Karyopherins, including at least 7 importin  $\alpha$  and 22 importin  $\beta$  proteins, are an evolutionarily conserved family of transport factors responsible for nucleocytoplasmic transport.<sup>1,2</sup> Except for some proteins that can be imported by directly binding to importin  $\beta$ , numerous cargo proteins rely on specific importin  $\alpha$  as adapters that interact with importin  $\beta$  and the nuclear pore complex. Typically, nucleocytoplasmic transport requires a classical nuclear localization signal on cargo proteins to interact with importin,<sup>3,4</sup> and this process is regulated by the Ran-GTP and Ran-GDP switches.<sup>5</sup> Aberrant nucleocytoplasmic transport of protein cargos leads to the pathogenesis of human diseases and developmental defects.<sup>6-8</sup>

Karyopherin  $\alpha$ -2 (KPNA2, importin  $\alpha$ 1) participates in the regulation of differentiation, transcription, viral infection, the immune response, cellular maintenance, and carcinogenesis due to the diversity of its cargos such as p53, Myc, E2F1, and NF $\kappa$ B.<sup>9-11</sup> KPNA2 also localizes to the cell membrane to regulate cell proliferation by interacting with FGF1, suggesting that KPNA2 is not only a transporter.<sup>12</sup> Several cellular stresses, such as heat shock, radiation, and hydrogen peroxide ( $H_2O_2$ )-induced oxidative stress, induce KPNA2 retention in the nucleus due to Ran gradient collapse and other unknown mechanisms.<sup>13-15</sup> Specifically, Miyamoto et al. discovered that KPNA2 remained in the nucleus after stress exposure, even when RanGTP was injected into the nucleus to supply nuclear Ran.<sup>13-15</sup>  $H_2O_2$ , a reactive oxygen species (ROS), is a classic intracellular signaling molecule involved in multiple kinase-driven pathways, including the alpha serine/threonine-protein kinase 1 (AKT1), the mammalian target of rapamycin (mTOR), AMP-activated protein kinase (AMPK), and Ataxia-telangiectasia mutated kinase (ATM) pathways,<sup>16-19</sup> and is involved in the regulation of multiple cell fates.<sup>16,20</sup> Endogenous  $H_2O_2$  is considered a second messenger that maintains cellular homeostasis, and high ROS levels cause protein damage via site-specific modifications and DNA damage.<sup>21,22</sup> On the other hand, exogenous ROS are induced when cells are exposed to environmental triggers, including UV radiation, genotoxins, and drugs.<sup>23</sup>  $H_2O_2$ -induced nuclear retention of KPNA2 has been reported to affect gene expression by binding to DNase I-sensitive nuclear components,<sup>13,14</sup> supporting an unconventional role for nuclear KPNA2 in regulating gene transcription. However, the molecular mechanisms underlying the oxidative stress-induced nuclear retention of KPNA2 remain unclear.

We herein identified AKT1 signaling as a critical factor leading to the nuclear accumulation of KPNA2 in

response to  $H_2O_2$ -induced oxidative stress. We showed that the phosphorylation of KPNA2 at S62 was a crucial post-translational modification involved in regulating the nucleocytoplasmic distribution and complex formation of KPNA2-NPM1 for modulating gene transcription. Cyclin-dependent kinase 1 (CDK1) mediated KPNA2 S62 phosphorylation and promoted the nuclear export of KPNA2. Thus, we infer that AKT1 and CDK1 signaling regulate the homeostasis of phosphorylated KPNA2 at S62 in the cytoplasmic and nuclear compartments, thereby maintaining cyclic nucleocytoplasmic shuttling of KPNA2 under oxidative stress.

## 2 | MATERIALS AND METHODS

### 2.1 | Cell culture

Human cervical cancer HeLa cells were purchased from the Food Industry Research and Development Institute (Hsinchu, Taiwan) and cultured in Dulbecco's modified Eagle's medium (DMEM; Gibco, Invitrogen, Carlsbad, CA, USA). The medium contained 10% fetal bovine serum (FBS) (Gibco), 100 units/mL penicillin-streptomycin (Gibco), and 2 mM L-glutamine (Gibco). Cells were maintained at 37°C in a humidified atmosphere of 95% air/5%  $CO_2$ . For stable isotope labeling by amino acids in cell culture (SILAC)-labeled proteomic analysis, HeLa cells were cultured as described previously.<sup>24</sup> Briefly, light HeLa cells were maintained in arginine- and lysine-depleted DMEM supplemented with 10% dialyzed FBS (Gibco) and 0.1 mg/mL light L-lysine and L-arginine. Heavy HeLa cells were maintained in medium supplemented with 0.1 mg/mL heavy L-lysine and L-[U-<sup>13</sup>C<sub>6</sub>]arginine (Sigma-Aldrich, St. Louis, MO, USA). Cell cultures were determined to be *Mycoplasma* free by DNA fluorochrome staining with Hoechst 33258 bisbenzimidazole. Short tandem repeat (STR) profiling was utilized to authenticate all the cell lines.

### 2.2 | Antibodies and reagents

All commercial antibodies used in this study are listed in Table S1-S2. An anti-phosphorylated KPNA2 S62 antibody was raised against a peptide of human KPNA2 (<sup>55</sup>SFPDDAT[pSer]PLQENRNC<sup>70</sup>) and kindly provided by Professor Fang-Jen S. Lee (National Taiwan University, Taipei, Taiwan). Kinase inhibitors, including the AKT inhibitor wortmannin (681675), the AMPK inhibitor compound C (171260), and the ATM inhibitor Ku55933 (118500), were purchased from Millipore (Billerica, MA, USA). The mTOR inhibitor everolimus (ab142151) was purchased from Abcam (Cambridge, MA, USA). The

CDK1 inhibitor RO-3306 (SML-0569) was purchased from Sigma–Aldrich (MA, USA).

### 2.3 | Small interfering RNA (siRNA) transfection

Cells were transfected with negative control siRNA (NC siRNA) or siRNAs against AKT1 (Dharmacon, Lafayette, USA), KPNA2 (GeneXBio, Helix Technology Co., Ltd., Taiwan), or nucleophosmin 1 (NPM1) (GeneXBio) with Lipofectamine RNAiMAX transfection reagent (Invitrogen, Carlsbad, California, USA) in OPTI-MEM. The sequences of the siRNAs used in this study are listed in Table S2.

### 2.4 | Plasmid constructs

The wild-type (WT) KPNA2-Myc construct was generated in our previous study.<sup>11</sup> Site-directed mutagenesis of KPNA2 (phospho-mimetic KPNA2-S62E and phospho-deficient KPNA2-S62A) was performed using the QuikChange Lightning Multi Site-Directed Mutagenesis Kit (Agilent Technologies, Santa Clara, CA, USA) according to the manufacturer's instructions. The mutated products were verified by direct DNA sequencing.

### 2.5 | Immunofluorescence assay (IFA) and image quantification

The cells were seeded on coverslips, fixed with 4% formaldehyde for 15 min and permeabilized in 0.1% Triton X-100/0.05% SDS/PBS for 5 min. The slides were blocked in 0.2% BSA/0.1% saponin/PBS and then incubated with primary antibodies in blocking solution. After being washed, the slides were incubated with Alexa Fluor-conjugated secondary antibodies (Molecular Probes, California, USA) and Hoechst 33258 (Molecular Probes) in blocking solution in the dark. The slides were mounted in 90% glycerol/10%  $\rho$ -phenylenediamine/PBS. Images were acquired using a Zeiss ApoTome fluorescence microscope and AxioVision Rel 4.9 software (Carl Zeiss, Gottingen, Germany). KPNA2 translocation was analyzed by using IN Cell 1000 analyzer software (Agilent Technologies) and ZEN Blue software (ZEISS, Oberkochen, Germany).

### 2.6 | Subcellular fractionation assay

The cells were seeded in 10-cm petri dishes and grown to 80% confluence. The cells were harvested by

trypsinization, and the cell pellets were fractionated using an NE-PER Nuclear and Cytoplasmic Extraction Reagent Kit (Cat. 78,833, Thermo Fisher Scientific, Lafayette) or a Nuclear Extraction Kit (ab113474, Abcam) according to the manufacturer's instructions. The fractionation efficacy was confirmed by Western blotting using specific antibodies against  $\alpha$ -tubulin (cytoplasmic marker) and lamin B1 (nuclear marker).

### 2.7 | Immunoprecipitation (IP) assay

HeLa cell lysates were incubated with the anti-KPNA2 antibody and Dynabeads® Protein G (Invitrogen) for 2 h at room temperature as described previously.<sup>24</sup> The immunoprecipitated products were collected and sequentially washed with Tris/Dithiothreitol (DTT)/NaCl wash buffer (20 mM Tris–HCl pH 7.0, 0.5 mM DTT, 250 mM NaCl) and Tris/DTT wash buffer (20 mM Tris–HCl (pH 7.0), 0.5 mM DTT). The Dynabeads were boiled in sample buffer for subsequent SDS–PAGE and Western blotting or silver staining.

### 2.8 | Western blotting

Western blotting was performed as previously described.<sup>25</sup> Proteins were separated by SDS–PAGE and then transferred to polyvinylidene difluoride membranes. The indicated targets were examined with primary antibodies and HRP-conjugated secondary antibodies in a Tris–NaCl–Tween system. The protein signals were evaluated with chemiluminescent HRP substrates (Merck Millipore).

### 2.9 | In-gel protein digestion

Gel bands were excised from SDS–PAGE and digested with trypsin (1:100; Promega, Madison, WI) as described previously.<sup>24</sup> The peptides were extracted and dried in a SpeedVac vacuum concentrator and stored at  $-80^{\circ}\text{C}$ .

### 2.10 | Quantitative proteomics analysis

For quantitative proteomics analysis, liquid chromatography–tandem mass spectrometry (LC–MS/MS) analysis was performed as previously described.<sup>26</sup> For quantitative phosphoproteome analysis, the corresponding heavy peptides and light peptides were mixed, suspended and acidified in 2% formic acid/40% acetonitrile. The phosphopeptides were enriched by a titanium dioxide trap column (GL Sciences, 10  $\mu\text{m}$ ,

0.3 × 5 mm), and the tandem mass spectrometry experiments were performed on an LTQ-Orbitrap Elite Hybrid MS spectrometer (Thermo Fisher Scientific) operated with Xcalibur 2.2 software (Thermo Fisher Scientific). The *m/z* scan range for the MS scans was 350–2000 Da. Phosphopeptides were examined by neutral loss scanning. The resulting mass spectra were searched using the Swiss-Prot human sequence database with the Mascot search engine (Matrix Science, London, UK, version 2.2.04). The raw spectrometry data were analyzed by Proteome Discoverer software (version 1.4, Thermo Fisher Scientific, San Jose, CA) with a precursor ion quantifier node for SILAC quantification and phosphoRS site probabilities for phosphorylation site assignment.

### 2.11 | Proximity ligation assay (PLA)

The PLA was carried out with a Duolink® In Situ Red Starter Kit Mouse/Rabbit (Sigma–Aldrich, DUO92101). Briefly, HeLa cells were seeded on coverslips, treated with 1 mM H<sub>2</sub>O<sub>2</sub> for 30 min, fixed in 500 μL of 4% paraformaldehyde/PBS for 15 min at room temperature and permeabilized in 500 μL of 0.1% Triton X-100/0.05%/PBS for 5 min. Images were acquired using a Zeiss ApoTome fluorescence microscope and AxioVision Rel 4.9 software (Carl Zeiss, Göttingen, Germany).

### 2.12 | Statistical analysis

The quantitative data are shown as the mean ± standard deviation (SD) and were analyzed using GraphPad Prism 8.0.2 software (GraphPad Software). For comparisons between two groups, an unpaired Student's *t*-test or Mann–Whitney test was used. For comparisons among more than two groups, one-way ANOVA with Tukey's test or Dunnett's test was used. *P* values less than 0.05 (*p* < 0.05) indicated statistical significance.

## 3 | RESULTS

### 3.1 | H<sub>2</sub>O<sub>2</sub>-induced AKT1 activation regulates the accumulation of KPNA2

To confirm the nuclear translocation of KPNA2 under oxidative stress, we first used an immunofluorescence assay and image quantification to show that H<sub>2</sub>O<sub>2</sub> induced KPNA2 localization to the nucleus in a dose- and time-dependent manner (Figure S1–S6). The enriched nuclear fractions of KPNA2 were observed in cells treated

with 0.5 mM or 1 mM H<sub>2</sub>O<sub>2</sub> for 15–60 min. A lower dose of H<sub>2</sub>O<sub>2</sub> (0.2 mM) induced the nuclear distribution of KPNA2 after 30–60 min. To determine which signaling pathway is responsible for the H<sub>2</sub>O<sub>2</sub>-induced nuclear translocation of KPNA2, we treated cells with H<sub>2</sub>O<sub>2</sub> and AKT, mTOR, AMPK, and ATM kinase inhibitors. We first observed that the AKT inhibitor decreased H<sub>2</sub>O<sub>2</sub>-induced nuclear accumulation of KPNA2 and phosphorylation of AKT (Figure 1A,B). The mTOR, AMPK, and ATM inhibitors did not reduce KPNA2 accumulation in the nucleus under H<sub>2</sub>O<sub>2</sub>-induced oxidative stress, although mTOR and ATM inhibitors had a minor effect on H<sub>2</sub>O<sub>2</sub>-induced AKT phosphorylation (Figure S2). We also showed that AKT1 knockdown reduced H<sub>2</sub>O<sub>2</sub>-induced nuclear accumulation of KPNA2 in HeLa cells (Figure 1C,D) and in MDA-MB-231 breast cancer cells (Figure S3). These results suggest that AKT1 activation plays a critical role in H<sub>2</sub>O<sub>2</sub>-induced nuclear retention of KPNA2.

### 3.2 | Reducing KPNA2 S62 phosphorylation promotes its nuclear distribution in response to H<sub>2</sub>O<sub>2</sub>

KPNA2 can be phosphorylated at many sites, and phosphorylation at serine 105 has been shown to regulate the nucleocytoplasmic distribution of KPNA2 and its cargo in a cell type-specific manner.<sup>27,28</sup> To determine the phosphorylation sites related to H<sub>2</sub>O<sub>2</sub>-induced nuclear distribution of KPNA2, we used a SILAC-based quantitative proteomics approach combined with subcellular fractionation and KPNA2 immunoprecipitation to analyze the differential phosphorylation of KPNA2 in control cells and H<sub>2</sub>O<sub>2</sub>-treated cells (Figure 2A). A reduction of phosphorylated serine 62 (S62) on KPNA2 was detected in the cytoplasmic fraction of H<sub>2</sub>O<sub>2</sub>-treated cells, but this phosphorylation was not identified in the nuclear fraction (Figure S4). We raised phospho-specific polyclonal antibodies against phosphorylated S62 of KPNA2 and confirmed their specificity by Western blotting using WT, phospho-mimetic (KPNA2-S62E), and phospho-deficient (KPNA2-S62A) KPNA2 mutants produced by HeLa cells and *E. coli* (Figure S5). Consistent with the quantitative results of our mass spectrometry analysis, H<sub>2</sub>O<sub>2</sub> decreased the level of S62 phosphorylated on KPNA2 (Figure 2B). IFA also showed that in unstressed cells, exogenously expressed WT KPNA2 and the phosphomimetic KPNA2-S62E were preferentially distributed in the cytoplasm. However, the phospho-deficient KPNA2-S62A mutant was significantly enriched in the nuclear fraction (Figure 2C,D). These results suggest that S62 phosphorylation is involved in regulating the nucleocytoplasmic shuttling of KPNA2, and H<sub>2</sub>O<sub>2</sub> reduces the phosphorylation of KPNA2 S62 to promote its nuclear entry.

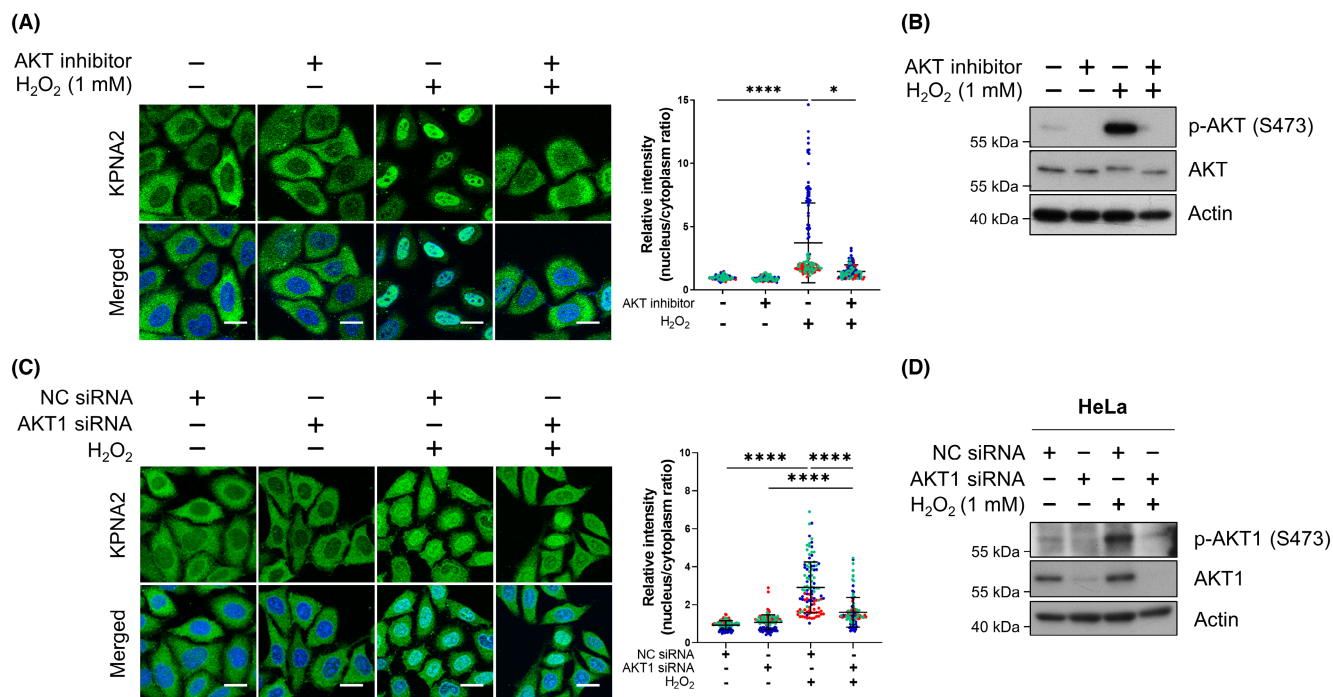


**FIGURE 1** AKT1 activation regulates H<sub>2</sub>O<sub>2</sub>-induced KPNA2 accumulation. (A) IFA of KPNA2 in HeLa cells treated with 5  $\mu$ M wortmannin (AKT inhibitor) for 2 h, and/or H<sub>2</sub>O<sub>2</sub> for 30 min. (C) IFA of KPNA2 in HeLa cells transfected with negative control siRNA (NC) and AKT1 siRNA and exposed to 1 mM H<sub>2</sub>O<sub>2</sub> for 30 min. Left panel: Representative images. Nuclei were counterstained with Hoechst 33258. Scale bars, 20  $\mu$ m. Right panel: Quantification of the nuclear/cytoplasmic ratios of KPNA2 staining ( $n > 100$  cells for each group). One data point represents one cell. Data are presented as means  $\pm$  SDs of three independent experiments, with each color representing data from an independent experiment. \* $p < 0.05$ , \*\*\*\* $p < 0.0001$  based on one-way ANOVA with Tukey's test. (B, D) Protein expression was analyzed by Western blotting with protein- and phosphorylation-specific antibodies as indicated. Actin was used as a loading control.

### 3.3 | The AKT1-CDK1 axis regulates the homeostasis of KPNA2 S62 phosphorylation in nucleocytoplasmic compartments

A recent study showed that CDK1 was a kinase that acted on KPNA2 S62, and KPNA2 S62 was phosphorylated during mitosis, which regulated mitotic spindle assembly.<sup>29,30</sup> Considering that the shuttling of KPNA2 between nuclear and cytoplasmic compartments is critical for the maintenance of its transport function, we reasoned that AKT1 activation and dephosphorylation of S62 contribute to the nuclear import of KPNA2 and that CDK1 kinase-dependent phosphorylation on KPNA2 S62 is involved in its nuclear export. To test this hypothesis, we treated cells with the CDK1 inhibitor RO-3306 and observed an increase in endogenous KPNA2 signals in the nuclear fraction (Figure 3A). Western blotting revealed reduced phosphorylation of KPNA2 S62 in cells treated with a CDK1 inhibitor, and CDK1 inactivation resulted in an increase in the level of the inhibitory phosphorylation of CDK1 at tyrosine 15 (Y15) (Figure 3B). Time course experiments further showed that H<sub>2</sub>O<sub>2</sub> induced AKT1 activation, followed by reduced KPNA2 S62 phosphorylation, and then activated

CDK1 (Figure 3C). To clarify this phenomenon, we address two questions: first, we investigated whether AKT1 regulates KPNA2 S62 phosphorylation, and second, whether AKT1 regulates CDK1 activity in response to oxidative stress. We found that AKT1 knockdown increased phosphorylation of KPNA2 S62 with or without the presence of H<sub>2</sub>O<sub>2</sub>. AKT1 knockdown also caused inactivation of CDK1, with increased levels of phosphorylated Y15 on CDK1. Notably, AKT1 knockdown still increased KPNA2 S62 phosphorylation in cells treated with CDK1 inhibitor (Figure 3D). These results suggest that the AKT1-CDK1 axis regulates the KPNA2 S62 phosphorylation to maintain the cyclic nucleocytoplasmic transport of KPNA2.

### 3.4 | H<sub>2</sub>O<sub>2</sub>-induced AKT1 signaling promotes the KPNA2-NPM1 interaction and regulates CCND1 transcription in the nucleus

KPNA2 participates in the regulation of cellular processes through its transporter role. To clarify the proteins that differentially interact with KPNA2 under

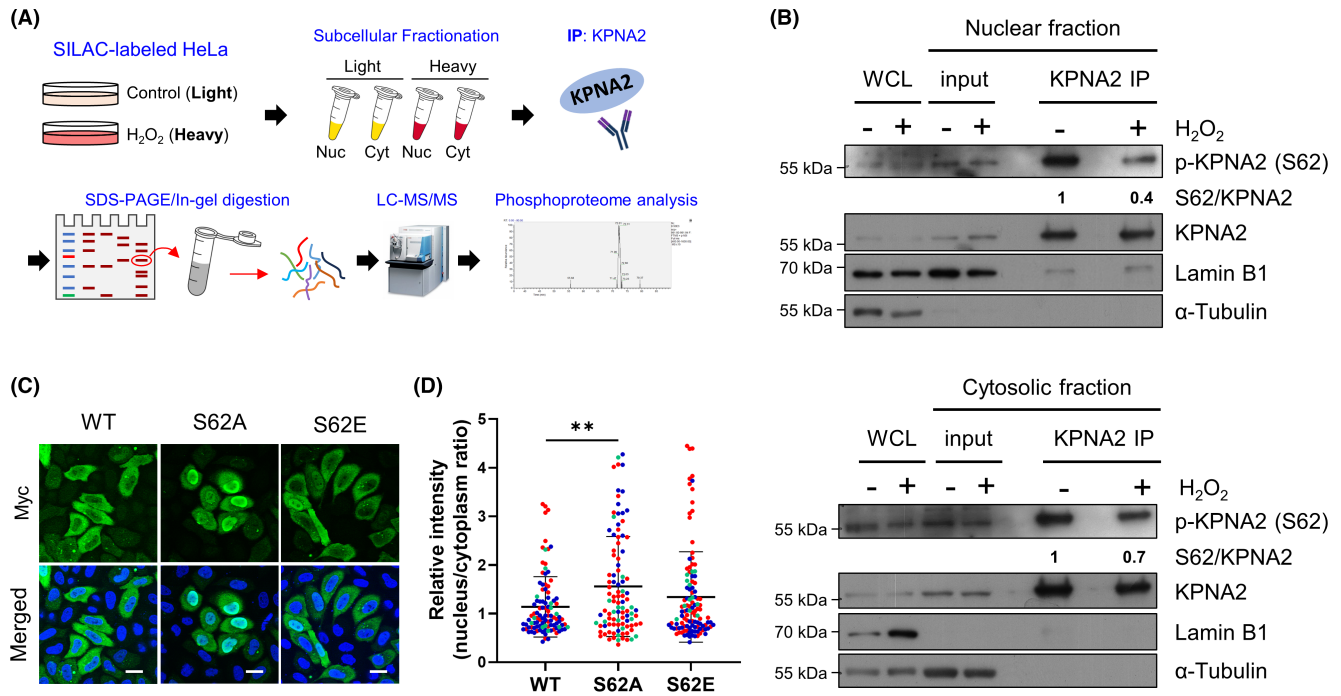


**FIGURE 2** Reducing S62 phosphorylation of KPNA2 promotes its nuclear distribution in response to H<sub>2</sub>O<sub>2</sub>. (A) Schematic of a SILAC-based quantitative proteomics approach coupled with subcellular fractionation and immunoprecipitation (IP) to examine H<sub>2</sub>O<sub>2</sub>-induced KPNA2 phosphorylation and the KPNA2 interactome. (B) The reduction in KPNA2 S62 phosphorylation in the nuclear and cytosolic fractions was verified by IP and Western blotting using an anti-phospho-KPNA2 antibody (p-KPNA2 (S62)). Lamin B1 and α-tubulin were used as nuclear and cytoplasmic loading controls, respectively. Representative images and quantifications are shown. (C) The phospho-deficient KPNA2-S62A mutant was enriched in the nuclear fraction. HeLa cells were transfected with Myc-tagged KPNA2-WT, KPNA2-S62A, or KPNA2-S62E plasmids for 24 h. Exogenous KPNA2 was labeled with an anti-Myc antibody (green). The cell nuclei were counterstained with Hoechst 33258. Scale bar, 20 μm. (D) Quantification of the nuclear/cytoplasmic ratios of exogenous KPNA2 staining ( $n > 100$  cells for each group). One data point represents one cell. Data are presented as the means  $\pm$  SDs of three independent experiments, with each color representing data from an independent experiment.  $***p < 0.01$  based on one-way ANOVA with Tukey's test.

H<sub>2</sub>O<sub>2</sub>-induced oxidative stress conditions, we identified proteins that interacted with nuclear KPNA2 via IP coupled with a quantitative proteomics approach. We identified a nucleolar phosphoprotein NPM1 as a KPNA2-interacting protein in response to H<sub>2</sub>O<sub>2</sub> by mass spectrometry (Figure 4A). Western blot analysis of the IP products confirmed that H<sub>2</sub>O<sub>2</sub> increased the interaction of NPM1 with nuclear KPNA2. Consistently, NPM1 interacted less with cytosolic KPNA2 after H<sub>2</sub>O<sub>2</sub> exposure (Figure 4B). Compared to the corresponding inputs from unstressed and H<sub>2</sub>O<sub>2</sub>-treated cells, the NPM1 ratios detected in nuclear and cytoplasmic KPNA2 IP products were 0.13 and 0.18, respectively. This observation supports the theory that KPNA2 acts as a carrier to initiate the binding and nuclear translocation of its cargo NPM1, in the cytoplasmic fraction of unstressed cells. PLA experiments further demonstrated a direct interaction between KPNA2 and NPM1 in cells, where the KPNA2-NPM1 complex was mainly distributed in the cytoplasm of unstressed cells; however, this interaction in the nucleus was significantly enhanced after H<sub>2</sub>O<sub>2</sub> treatment (Figure 4C). NPM1 is known to be involved in

intracellular oxidative stress, but the role and regulatory mechanism of NPM1 in oxidative stress is unclear.<sup>31</sup> We demonstrated that AKT1 knockdown impaired the H<sub>2</sub>O<sub>2</sub>-induced KPNA2-NPM1 interaction and increased the abundance of KPNA2 S62 phosphorylation in the IP product compared with control cells treated with siRNA (Figure 4D). We also investigated whether KPNA2 or NPM1 can regulate each other's nuclear translocation. As shown in Figure 5A, KPNA2 knockdown significantly decreased the nuclear localization of NPM1 in cells treated with or without H<sub>2</sub>O<sub>2</sub>. NPM1 knockdown did not alter the nuclear distribution of KPNA2, but caused large granule formation of KPNA2 in the cytoplasm and resulted in cells with multiple or fragmented nuclei (Figure S6). We observed cell death in HeLa cells after H<sub>2</sub>O<sub>2</sub> treatment extended to 24 h (data not shown). Our previous studies also showed that KPNA2 knockdown resulted in G2/M phase arrest in lung cancer and breast cancer cells.<sup>24</sup> Cyclin D1 (CCND1) is an important regulator of cell cycle progression, acts as a transcriptional coregulator, and has been reported as an NPM1 target gene.<sup>32,33</sup> We then examined the CCND1

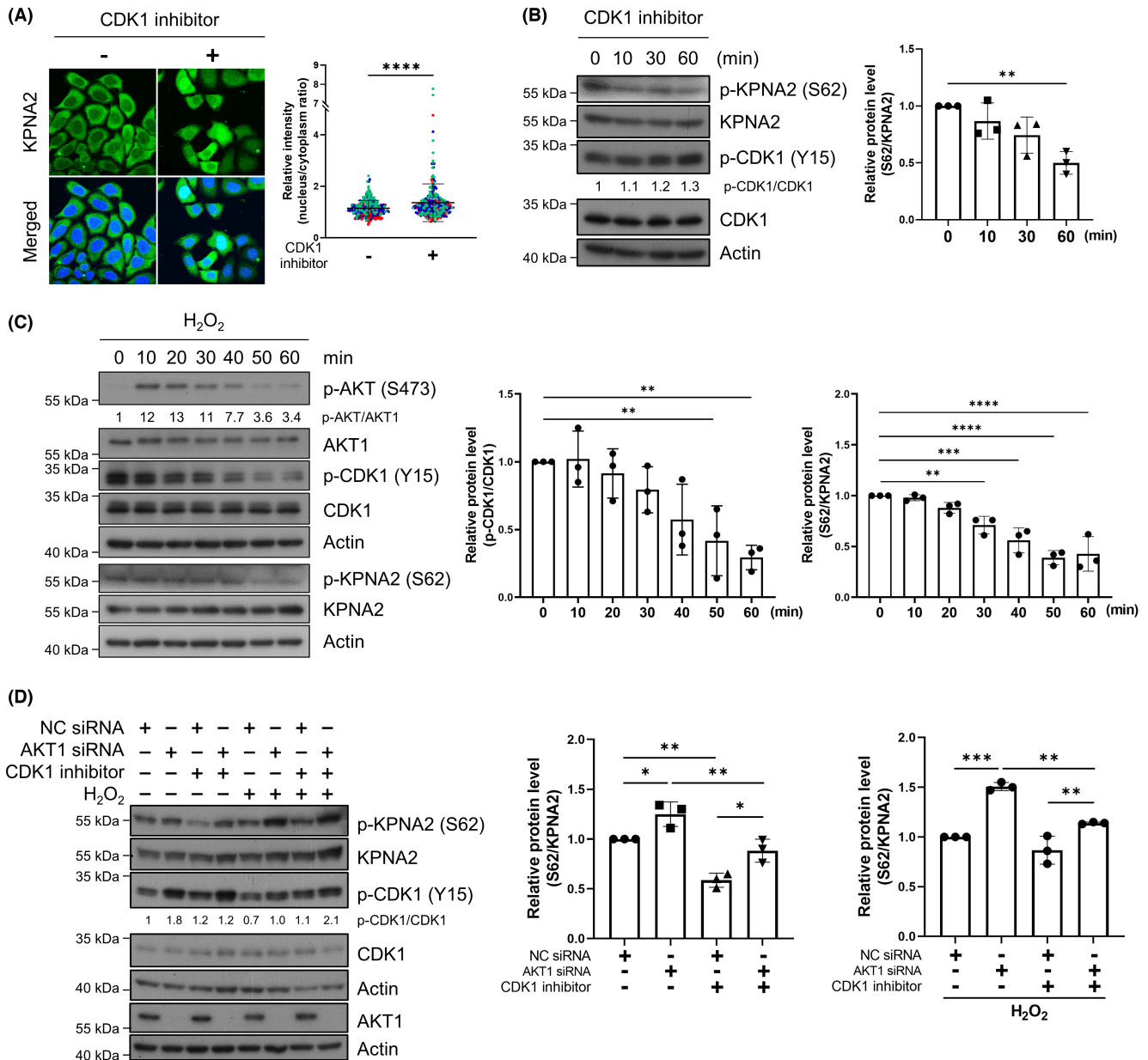


**FIGURE 3** The AKT1-CDK1 axis regulates the homeostasis of KPNA2 phosphorylation in nucleocytoplasmic compartments. (A) Treatment with CDK1 inhibitors increased the amount of endogenous KPNA2 in the nuclear fraction. KPNA2 expression in CDK1 inhibitor RO-3306-treated HeLa cells was analyzed by IFA. Left panel: Representative images. The cell nuclei were counterstained with Hoechst 33258. Scale bar, 20  $\mu$ m. Right panel: Quantification of the nuclear/cytoplasmic ratios of KPNA2 staining ( $n > 250$  cells for each group). One data point represents one cell. Data are presented as the means  $\pm$  SDs of three independent experiments, with each color representing data from an independent experiment. \*\*\*\* $p < 0.0001$  based on Mann-Whitney test. (B) CDK1 inhibition reduced the level of phosphorylated S62 on KPNA2. Western blot analysis of the indicated proteins in CDK1 inhibitor-treated cells after 10, 30 and 60 min. Data are presented as the means  $\pm$  SDs of three independent experiments. \*\* $p < 0.01$  based on one-way ANOVA with Dunnett's test. (C) H<sub>2</sub>O<sub>2</sub> induced AKT1 activation followed by a decrease of KPNA2 S62 phosphorylation and activation of CDK1. Western blot analysis of the indicated proteins in cells exposed to H<sub>2</sub>O<sub>2</sub> for 10–60 min. The data are presented as the means  $\pm$  SDs of three independent experiments. \*\* $p < 0.01$ , \*\*\* $p < 0.001$ , \*\*\*\* $p < 0.0001$  based on one-way ANOVA with Dunnett's test. (D) HeLa cells were transfected with AKT siRNA for 48 h and then treated with H<sub>2</sub>O<sub>2</sub> and a CDK1 inhibitor. The expression of the indicated proteins was examined by Western blotting. Actin was used as a loading control. Representative images and quantifications are shown. Data are presented as the means  $\pm$  SDs of three independent experiments. \* $p < 0.05$ , \*\* $p < 0.01$ , \*\*\* $p < 0.001$  based on one-way ANOVA with Tukey's test.

expression in KPNA2- and NPM1-knockdown cells. Knockdown of KPNA2 and NPM1 indeed reduced the transcription of CCND1 (Figure 5B). CCND1 mRNA

levels were also reduced by H<sub>2</sub>O<sub>2</sub> treatment. These results suggest that in response to oxidative stress, S62 phosphorylation of KPNA2 is involved in the formation

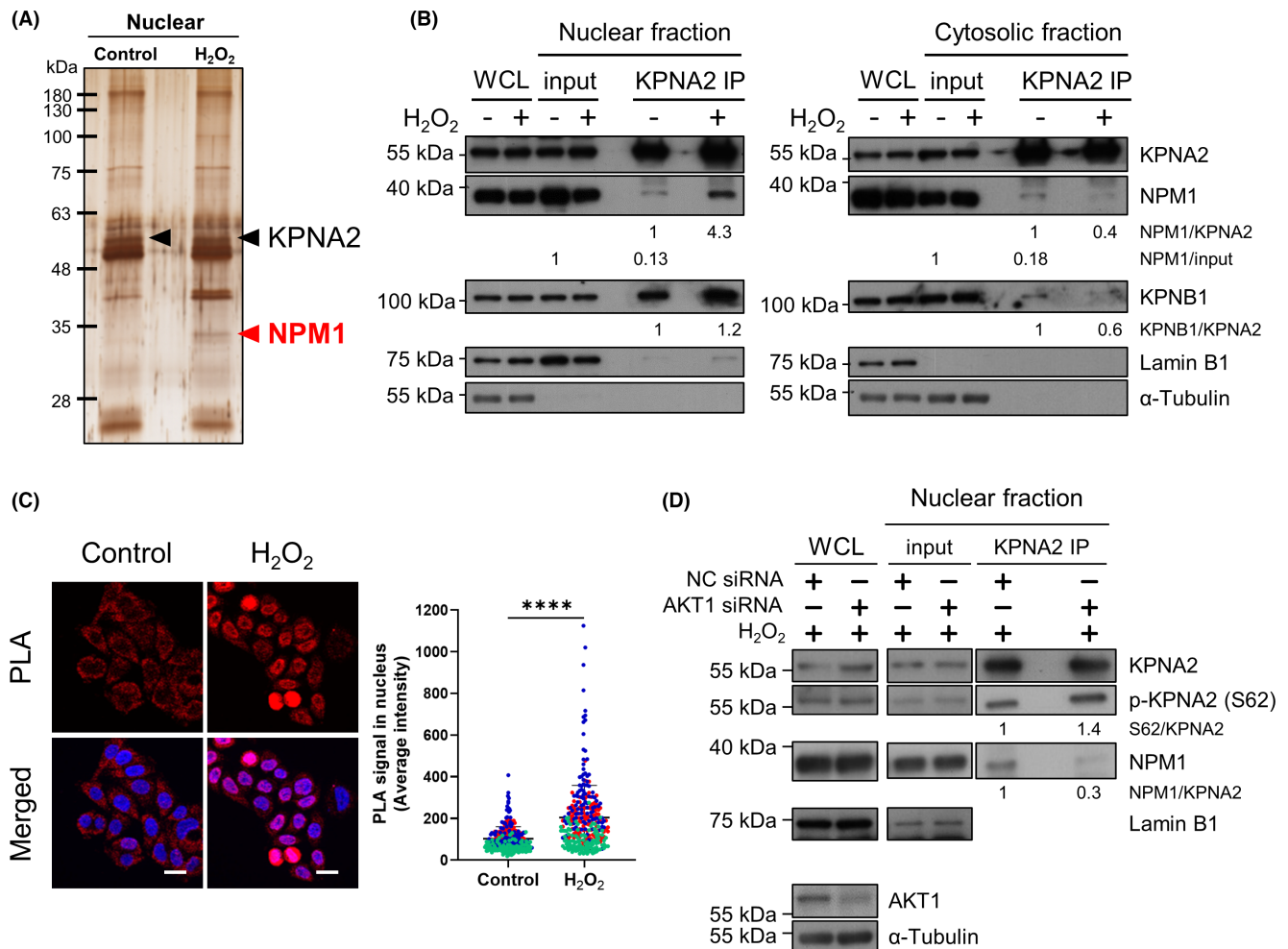
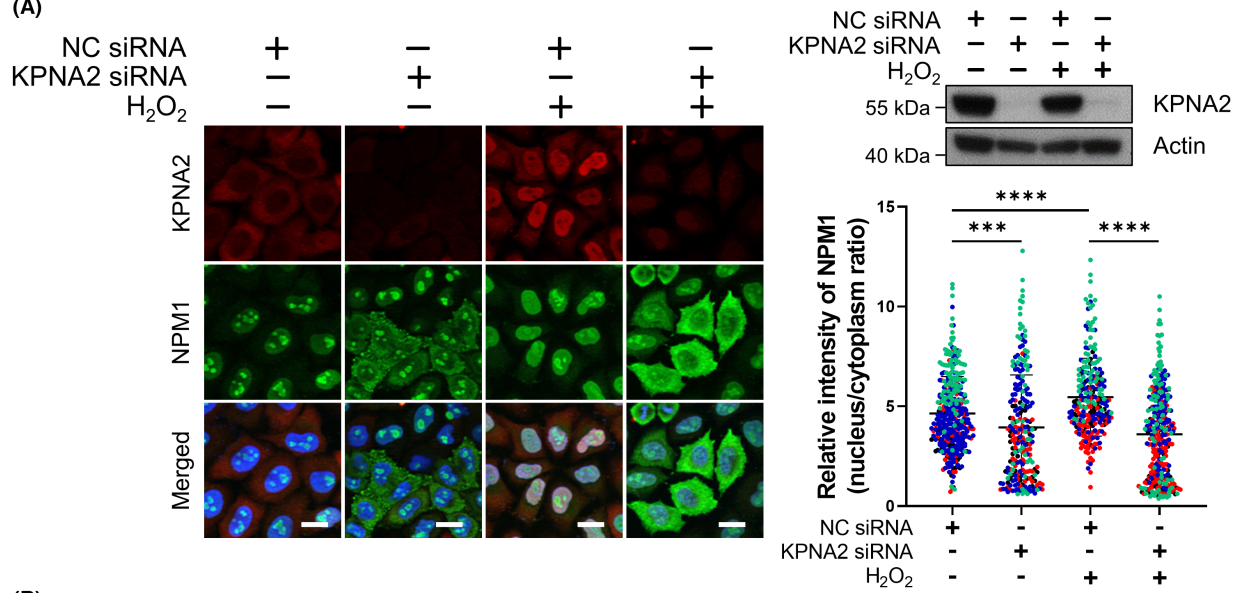


**FIGURE 4** H<sub>2</sub>O<sub>2</sub>-mediated activation of AKT1 signaling promotes KPNA2-NPM1 interactions in the nucleus. (A) Silver-stained gel showing the immunoprecipitated nuclear KPNA2 protein complex. The nuclear IP products were separated by 10% SDS-PAGE followed by in-gel digestion and LC-MS/MS analysis. The differential band of NPM1 induced by H<sub>2</sub>O<sub>2</sub> is indicated by a red arrow. (B) Validation of nuclear and cytosolic KPNA2-interacting proteins by subcellular fractionation, IP and Western blotting. Equal amounts (1%) of whole cell lysate (WCL) and nuclear or cytoplasmic fractions used for IP were separated in 10% SDS-PAGE and subjected to Western blotting analysis. Lamin B1 and  $\alpha$ -tubulin were used as nuclear and cytosolic loading controls, respectively. (C) In situ PLA of the interaction between KPNA2 and NPM1 in H<sub>2</sub>O<sub>2</sub>-treated HeLa cells. Left panel: Representative images. Nuclei were counterstained with Hoechst 33258. Scale bars, 20  $\mu$ m. Right panel: Quantification of PLA signals in the nuclear fraction ( $n > 250$  from each group). One data point represents one cell. The data are presented as the means  $\pm$  SDs of three independent experiments, with each color representing data from an independent experiment. \*\*\*\* $p < 0.0001$  based on an unpaired Student's *t*-test. (D) AKT1 knockdown reduced the H<sub>2</sub>O<sub>2</sub>-induced KPNA2-NPM1 interaction, which was accompanied by an increase in the level of phosphorylated S62 in nuclear KPNA2. HeLa cells were transfected with AKT1 siRNA and exposed to 1 mM H<sub>2</sub>O<sub>2</sub> for 30 min, followed by subcellular fractionation and immunoprecipitation. The expression of the indicated proteins was examined by Western blotting.

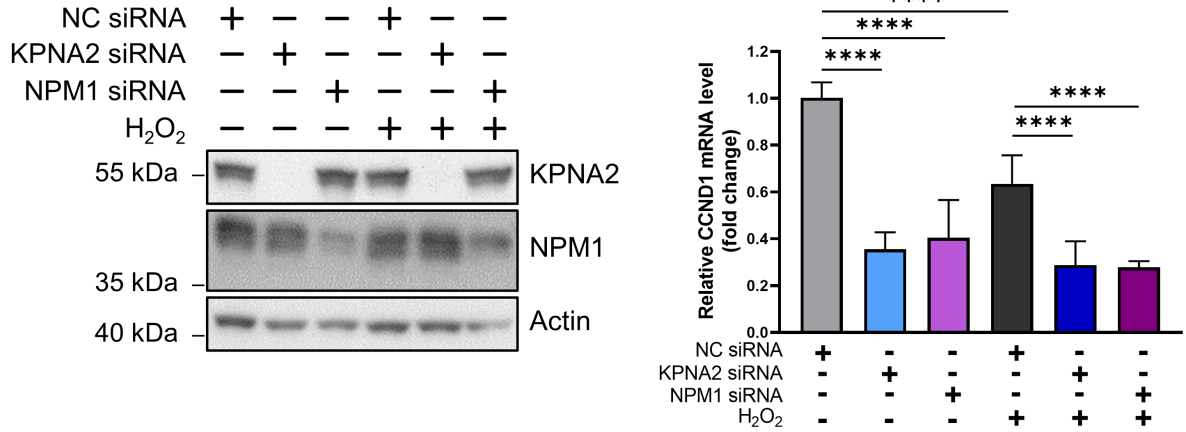
**FIGURE 5** Knockdown of KPNA2 and NPM1 reduces the transcription of CCND1. (A) NPM1 in KPNA2-knockdown cells treated with or without 1 mM H<sub>2</sub>O<sub>2</sub> for 30 min. Nuclei were counterstained with Hoechst 33258. Scale bars, 20  $\mu$ m. The quantification of the nuclear/cytoplasmic ratios of NPM1 staining ( $n > 200$  cells for each group) is presented. One data point represents one cell. The data are presented as the means  $\pm$  SDs of three independent experiments, with each color representing data from an independent experiment. \*\*\* $p < 0.001$ , \*\*\*\* $p < 0.0001$  based on one-way ANOVA with Tukey's test. Western blotting was used to confirm the efficacy of KPNA2 knockdown. (B) HeLa cells were transfected with KPNA2 or NPM1 siRNA for 48 h and then exposed to 1 mM H<sub>2</sub>O<sub>2</sub>. The mRNA levels of CCND1 were determined by qRT-PCR. Gene knockdown efficacy was confirmed by Western blotting. \*\*\*\* $p < 0.0001$  based on one-way ANOVA with Tukey's test. (C) Working hypothesis: H<sub>2</sub>O<sub>2</sub> activates AKT1 and reduces the phosphorylation level of KPNA2 S62 by regulating undefined phosphatases, resulting in the nuclear translocation of KPNA2 (black dot arrow, thick). AKT1 also induces nuclear CDK1 activation, thereby phosphorylating S62 on KPNA2 and regulating its nuclear export (black dot arrow, thin). H<sub>2</sub>O<sub>2</sub> promoting nuclear entry of the KPNA2-NPM1 protein complex would attenuate NPM1-mediated CCND1 transcription under oxidative stress condition.



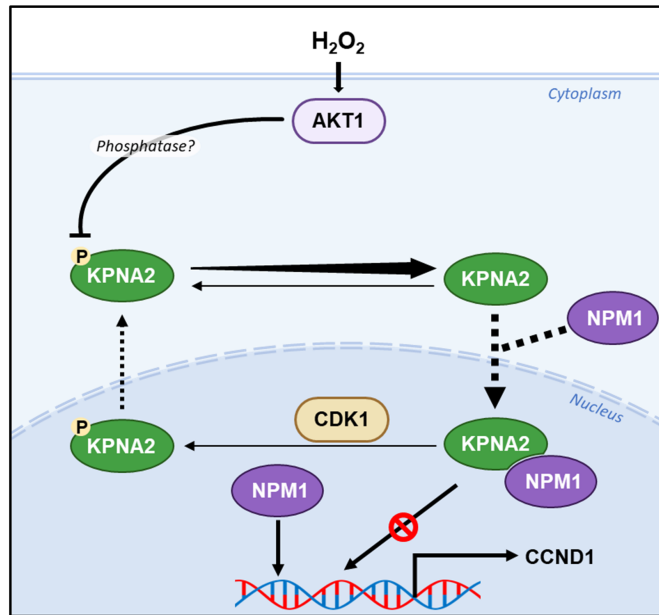
(A)



(B)



(C)



of a complex between KPNA2 and its cargo proteins, leading to regulation of gene transcription (Figure 5C).

## 4 | DISCUSSION

In this study, we show that oxidative stress mediates nucleocytoplasmic transport of KPNA2 via S62 phosphorylation regulated by the AKT1-CDK1 axis. We propose that once cells are exposed to oxidative stress, activated AKT1 initially induces unknown phosphatase activation to reduce phosphorylation of KPNA2 S62 and thereby promote nuclear entry of KPNA2, and that accumulation of dephosphorylated KPNA2 S62 in the nucleus can trigger activation of CDK1, which in turn phosphorylates KPNA2 S62 and promotes nuclear export of KPNA2. Since AKT1 knockdown increases KPNA2 S62 phosphorylation regardless of CDK1 inhibition, we argue that AKT1 activity is the critical factor in reducing KPNA2 S62 phosphorylation.

Our data showed that a low dose of H<sub>2</sub>O<sub>2</sub> (0.2 mM) promoted KPNA2 nuclear import after 30 min, and that a high dose of H<sub>2</sub>O<sub>2</sub> (0.5 mM and 1 mM) induced the KPNA2 nuclear accumulation in a time-dependent manner from 15-min treatments. We also observed that the p-AKT signal was strong after 10 min of H<sub>2</sub>O<sub>2</sub> exposure, but the signal weakened over time. These effects indicate that the dynamics of nucleocytoplasmic transport is tightly controlled under cellular stress conditions and are consistent with dynamic AKT activation in response to different stimulus intensities and periods. Generally, AKT activation occurs within 30 min of H<sub>2</sub>O<sub>2</sub> treatment in different cell types, followed by a significant attenuation of its activity.<sup>34,35</sup> For example, when C2C12 myoblast cells were exposed to 1 mM H<sub>2</sub>O<sub>2</sub>, phosphorylated AKT increased dramatically from 15 min to 2 h and decreased after 2 h.<sup>34</sup> In PC12 pheochromocytoma cells, 0.5 mM H<sub>2</sub>O<sub>2</sub> transiently activated AKT within 5–30 min and then inhibited AKT phosphorylation within 1–2 h.<sup>35</sup>

The current study demonstrates that the AKT1-CDK1 axis modulates nucleocytoplasmic transport of KPNA2 complexes in response to short-term exposure to H<sub>2</sub>O<sub>2</sub> by regulating phosphorylation of KPNA2. In mammalian cells, the tyrosine kinase Wee1-like protein kinase (WEE1Hu) phosphorylates CDK1 at Tyr15, thereby inhibiting CDK1 activity.<sup>36</sup> Katayama et al.<sup>37</sup> reported that AKT promoted G2/M cell cycle progression by phosphorylating WEE1Hu at Ser642, but WEE1Hu kinase activity was not affected by phosphorylation at Ser642. AKT abolished the effect of WEE1Hu by inducing the binding of phosphorylated WEE1Hu to 14–3-3σ and its translocation from the nucleus to the cytoplasm. Although the nuclear-to-cytoplasmic translocation of WEE1Hu in response to

H<sub>2</sub>O<sub>2</sub> remains to be verified, this result is consistent with our observations that AKT1 activity positively correlates with CDK1 activation in the nucleus (Figure 3C and Figure 5C).

One of the limitations of the current study is the specificity of the anti-phospho-antibodies used to detect KPNA2 S62 phosphorylation. The phospho-antibody showed high affinity for the KPNA2 S62E mutant but not for KPNA2-S62A or KPNA2-WT expression in HeLa cells (Figure S5B). However, this antibody could partially recognize the unphosphorylated recombinant KPNA2-WT produced by *E. coli* (Figure S5C), suggesting that this antibody had a low affinity for unphosphorylated S62 on KPNA2. Our data showed that CDK1 inhibitors were unable to completely abolish the KPNA2 phosphorylation signal detected by this anti-KPNA2 S62 phosphorylation antibody (Figure 3B). This observation suggests the possibility that kinases other than CDK1 phosphorylate KPNA2 at S62.

KPNA2 is currently considered a promising cancer biomarker and therapeutic target for many cancers.<sup>38–42</sup> High KPNA2 expression in cancers is associated with poor prognosis.<sup>10,43</sup> Nuclear accumulation of KPNA2 has been observed in cancer tissues of various origins, including lung adenocarcinoma tissues.<sup>9,42</sup> We reported that AKT1 knockdown attenuated the nuclear accumulation of KPNA2 in radioresistant lung cancer cells.<sup>44</sup> Our recent study found that acetylation of KPNA2 at lysine 22 and phosphorylation at serine 105 regulate the migration and nucleocytoplasmic distribution of KPNA2 in lung adenocarcinomas cells,<sup>27</sup> suggesting that post-translational modifications of KPNA2 are important in cancer biology. Based on mass spectrometry analyses, quantitative tissue phosphoproteome studies showed that KPNA2 phosphorylation at S62 was higher in breast cancer tissues<sup>45,46</sup> and colon cancer tissues<sup>47</sup> than in normal tissues. Therefore, the clinical and biological significance of KPNA2 S62 phosphorylation in oxidative stress-related pathogenesis and human diseases such as cancer should be investigated.

In the present study, we reported that H<sub>2</sub>O<sub>2</sub>-induced NPM1 interacts with KPNA2 in the nucleoplasm, and that this interaction is regulated by AKT1 activation and accompanied by a decrease in S62 phosphorylation, suggesting that phosphorylation modulates KPNA2 complex formation. NPM1 is a ubiquitously expressed nucleolar protein and a potential biomarker for lung adenocarcinoma, acute myeloid leukemia, and oral carcinoma.<sup>48–50</sup> NPM1 is involved in chromatin remodeling, genome stability, cell cycle progression, protein chaperones, apoptosis, and cell proliferation.<sup>51</sup> NPM1 has been reported to translocate to the nucleoplasm and stabilize p53 protein expression in response to H<sub>2</sub>O<sub>2</sub>-induced oxidative stress.<sup>31</sup> Recently, NPM1 was identified as a

protein associated with KPNA2 that promotes renal cell carcinogenesis.<sup>52</sup> Investigating which transcription factors and how KPNA2 modulates these transcription factors with the coregulator NPM1 to regulate gene expression profiles will provide insights cell fate mediated by KPNA2 in response to cellular stress.

In summary, we report that coordinated AKT1 and CDK1 signaling modulates phosphorylation of KPNA2 at S62, thereby regulating the nucleocytoplasmic distribution of KPNA2 and complex formation in response to H<sub>2</sub>O<sub>2</sub>-induced oxidative stress. This study also provides the basis for our understanding of the function of KPNA2 in adapting to oxidative stress through gene transcription for cell cycle regulation.

### AUTHOR CONTRIBUTIONS

J.-X. H. and C.-J. Y. conceptualization; J.-X. H., C.-I. W., C.-Y. K., T.-W. C., Y.-C. L. and T.-F. H. methodology; J.-X. H., C.-I. W., C.-Y. K. and C.-J. Y. investigation; J.-X. H. and C.-J. Y. writing-review and editing; C.-L. W. and C.-J. Y. funding acquisition and supervision; C.-J. Y. project administration.

### ACKNOWLEDGMENTS

This work was financially supported by grants from the National Science and Technology Council, Taiwan (105-2320-B-182-035-MY3 and 111-2320-B-182-019-MY3 to CJ Yu); the Chang Gung Memorial Hospital, Taoyuan, Taiwan (CMRPD1M0441-2 and BMRP894 to CJ Yu); and the Molecular Medicine Research Center, Chang Gung University, from The Featured Areas Research Center Program within the framework of the Higher Education Sprout Project by the Ministry of Education, Taiwan.

### CONFLICT OF INTEREST STATEMENT

The authors declare that they have no conflicts of interests.

### DATA AVAILABILITY STATEMENT

All the data are contained within the article and/or the supporting information. The mass spectrometry proteomics data have been deposited to the ProteomeXchange Consortium via the PRIDE partner repository<sup>53</sup> with the data set identifier PXD051121.

### ORCID


Jie-Xin Huang  <https://orcid.org/0009-0006-8992-1771>

Chun-I Wang  <https://orcid.org/0000-0001-8332-0162>

Ting-Wei Chang  <https://orcid.org/0009-0002-9926-0672>

Yu-Chin Liu  <https://orcid.org/0000-0002-2082-9647>

Ting-Feng Hsiao  <https://orcid.org/0000-0003-4074-9019>

Chih-Liang Wang  <https://orcid.org/0000-0003-2917-8307>

Chia-Jung Yu  <https://orcid.org/0000-0001-6301-7190>

### REFERENCES

1. Chook YM, Blobel G. Karyopherins and nuclear import. *Curr Opin Struct Biol.* 2001;11(6):703-715. doi:10.1016/S0959-440X(01)00264-0
2. Pumroy RA, Cingolani G. Diversification of importin-alpha isoforms in cellular trafficking and disease states. *Biochem J.* 2015;466(1):13-28. doi:10.1042/BJ20141186
3. Lu J, Wu T, Zhang B, et al. Types of nuclear localization signals and mechanisms of protein import into the nucleus. *Cell Commun Signal.* 2021;19(1):60. doi:10.1186/s12964-021-00741-y
4. Stewart M. Molecular mechanism of the nuclear protein import cycle. *Nat Rev Mol Cell Biol.* 2007;8(3):195-208. doi:10.1038/nrm2114
5. Sorokin AV, Kim ER, Ovchinnikov LP. Nucleocytoplasmic transport of proteins. *Biochemistry (Mosc).* 2007;72(13):1439-1457. doi:10.1134/S0006297907130032
6. Kosyna FK, Depping R. Controlling the gatekeeper: therapeutic targeting of nuclear transport. *Cells.* 2018;7(11):221. doi:10.3390/cells7110221
7. Wing CE, Fung HYJ, Chook YM. Karyopherin-mediated nucleocytoplasmic transport. *Nat Rev Mol Cell Biol.* 2022;23(5):307-328. doi:10.1038/s41580-021-00446-7
8. Wang W, Miyamoto Y, Chen B, et al. Karyopherin alpha deficiency contributes to human preimplantation embryo arrest. *J Clin Invest.* 2023;133(2):e159951. doi:10.1172/JCI159951
9. Christiansen A, Dyrskjot L. The functional role of the novel biomarker karyopherin alpha 2 (KPNA2) in cancer. *Cancer Lett.* 2013;331(1):18-23. doi:10.1016/j.canlet.2012.12.013
10. Han Y, Wang X. The emerging roles of KPNA2 in cancer. *Life Sci.* 2020;241:117140. doi:10.1016/j.lfs.2019.117140
11. Wang CI, Chien KY, Wang CL, et al. Quantitative proteomics reveals regulation of karyopherin subunit alpha-2 (KPNA2) and its potential novel cargo proteins in nonsmall cell lung cancer. *Mol Cell Proteomics.* 2012;11(11):1105-1122. doi:10.1074/mcp.M111.016592
12. Yamada K, Miyamoto Y, Tsujii A, et al. Cell surface localization of importin alpha1/KPNA2 affects cancer cell proliferation by regulating FGF1 signalling. *Sci Rep.* 2016;6:21410. doi:10.1038/srep21410
13. Yasuda Y, Miyamoto Y, Yamashiro T, et al. Nuclear retention of importin  $\alpha$  coordinates cell fate through changes in gene expression. *EMBO J.* 2012;31(1):83-94. doi:10.1038/emboj.2011.360
14. Miyamoto Y, Loveland KL, Yoneda Y. Nuclear importin alpha and its physiological importance. *Commun Integr Biol.* 2012;5(2):220-222. doi:10.4161/cib.19194
15. Miyamoto Y, Saiwaki T, Yamashita J, et al. Cellular stresses induce the nuclear accumulation of importin alpha and cause a conventional nuclear import block. *J Cell Biol.* 2004;165(5):617-623. doi:10.1083/jcb.200312008
16. Giorgio M, Trinei M, Migliaccio E, Pelicci PG. Hydrogen peroxide: a metabolic by-product or a common mediator of ageing signals? *Nat Rev Mol Cell Biol.* 2007;8(9):722-728. doi:10.1038/nrm2240

17. Bhattacharyya A, Chattopadhyay R, Mitra S, Crowe SE. Oxidative stress: an essential factor in the pathogenesis of gastrointestinal mucosal diseases. *Physiol Rev*. 2014;94(2):329-354. doi:10.1152/physrev.00040.2012
18. Sinenko SA, Starkova TY, Kuzmin AA, Tomilin AN. Physiological signaling functions of reactive oxygen species in stem cells: from flies to man. *Front Cell Dev Biol*. 2021;9:714370. doi:10.3389/fcell.2021.714370
19. Xie X, Zhang Y, Wang Z, et al. ATM at the crossroads of reactive oxygen species and autophagy. *Int J Biol Sci*. 2021;17(12):3080-3090. doi:10.7150/ijbs.63963
20. Kiran TR, Otlu O, Karabulut AB. Oxidative stress and antioxidants in health and disease. *J Lab Med*. 2023;47(1):1-11. doi:10.1515/labmed-2022-0108
21. Sharifi-Rad M, Anil Kumar NV, Zucca P, et al. Lifestyle, oxidative stress, and antioxidants: Back and forth in the pathophysiology of chronic diseases. *Front Physiol*. 2020;11:694. doi:10.3389/fphys.2020.00694
22. O'Flaherty C, Matsushita-Fournier D. Reactive oxygen species and protein modifications in spermatozoa. *Biol Reprod*. 2017;97(4):577-585. doi:10.1093/biolre/iox104
23. Afzal S, Abdul Manap AS, Attiq A, Albokhadaim I, Kandeel M, Alhojaily SM. From imbalance to impairment: the central role of reactive oxygen species in oxidative stress-induced disorders and therapeutic exploration. *Front Pharmacol*. 2023;14:1269581. doi:10.3389/fphar.2023.1269581
24. Wang CI, Wang CL, Wu YC, et al. Quantitative proteomics reveals a novel role of karyopherin alpha 2 in cell migration through the regulation of vimentin-pErk protein complex levels in lung cancer. *J Proteome Res*. 2015;14(4):1739-1751. doi:10.1021/pr501097a
25. Huang JX, Wu YC, Cheng YY, Wang CL, Yu CJ. IRF1 negatively regulates oncogenic KPNA2 expression under growth stimulation and hypoxia in lung cancer cells. *Onco Targets Ther*. 2019;12:11475-11486. doi:10.2147/OTT.S221832
26. Hsiao TF, Wang CL, Wu YC, et al. Integrative omics analysis reveals soluble Cadherin-3 as a survival predictor and an early monitoring marker of EGFR tyrosine kinase inhibitor therapy in lung cancer. *Clin Cancer Res*. 2020;26(13):3220-3229. doi:10.1158/1078-0432.CCR-19-3972
27. Feng HP, Liu YC, Wang CL, Liao WC, Yu JS, Yu CJ. Acetylation regulates the nucleocytoplasmic distribution and oncogenic function of karyopherin alpha 2 in lung adenocarcinoma. *Biochem Biophys Res Commun*. 2023;659:96-104. doi:10.1016/j.bbrc.2023.04.014
28. Nardozi JD, Lott K, Cingolani G. Phosphorylation meets nuclear import: a review. *Cell Commun Signal*. 2010;8:32. doi:10.1186/1478-811X-8-32
29. Guo L, Mohd KS, Ren H, et al. Phosphorylation of importin-alpha1 by CDK1-cyclin B1 controls mitotic spindle assembly. *J Cell Sci*. 2019;132(18):jcs232314. doi:10.1242/jcs.232314
30. Guo H, Wei JH, Zhang Y, Seemann J. Importin alpha phosphorylation promotes TPX2 activation by GM130 to control astral microtubules and spindle orientation. *J Cell Sci*. 2021;134(4):jcs258356. doi:10.1242/jcs.258356
31. Yang K, Wang M, Zhao Y, et al. A redox mechanism underlying nucleolar stress sensing by nucleophosmin. *Nat Commun*. 2016;7:13599. doi:10.1038/ncomms13599
32. Liu H, Huang J, Wang J, et al. Transvection mediated by the translocated cyclin D1 locus in mantle cell lymphoma. *J Exp Med*. 2008;205(8):1843-1858. doi:10.1084/jem.20072102
33. Coqueret O. Linking cyclins to transcriptional control. *Gene*. 2002;299(1-2):35-55. doi:10.1016/s0378-1119(02)01055-7
34. Pronsato L, Boland R, Milanese L. Testosterone exerts antiapoptotic effects against H<sub>2</sub>O<sub>2</sub> in C<sub>2</sub>C<sub>12</sub> skeletal muscle cells through the apoptotic intrinsic pathway. *J Endocrinol*. 2012;212(3):371-381. doi:10.1530/joe-11-0234
35. Chen L, Xu B, Liu L, et al. Hydrogen peroxide inhibits mTOR signaling by activation of AMPK $\alpha$  leading to apoptosis of neuronal cells. *Lab Invest*. 2010;90(5):762-773. doi:10.1038/labinvest.2010.36
36. Watanabe N, Broome M, Hunter T. Regulation of the human WEE1Hu CDK tyrosine 15-kinase during the cell cycle. *EMBO J*. 1995;14(9):1878-1891. doi:10.1002/j.1460-2075.1995.tb07180.x
37. Katayama K, Fujita N, Tsuruo T. Akt/protein kinase B-dependent phosphorylation and inactivation of WEE1Hu promote cell cycle progression at G2/M transition. *Mol Cell Biol*. 2005;25(13):5725-5737. doi:10.1128/MCB.25.13.5725-5737.2005
38. Sun Y, Li W, Li X, Zheng H, Qiu Y, Yang H. Oncogenic role of karyopherin  $\alpha$ 2 (KPNA2) in human tumors: a pan-cancer analysis. *Comput Biol Med*. 2021;139:104955. doi:10.1016/j.combiomed.2021.104955
39. Baschieri F, Confalonieri S, Bertalot G, et al. Spatial control of Cdc42 signalling by a GM130-RasGRF complex regulates polarity and tumorigenesis. *Nat Commun*. 2014;5:4839. doi:10.1038/ncomms5839
40. Gao L, Li Y, Yu C, et al. Oncogenic KPNA2 serves as a biomarker and immune infiltration in patients with HPV positive tongue squamous cell carcinoma. *Front Oncol*. 2022;12:847793. doi:10.3389/fonc.2022.847793
41. Huang L, Zhou Y, Cao XP, et al. KPNA2 is a potential diagnostic serum biomarker for epithelial ovarian cancer and correlates with poor prognosis. *Tumour Biol*. 2017;39(6):1010428317706289. doi:10.1177/1010428317706289
42. Wang CI, Wang CL, Wang CW, et al. Importin subunit alpha-2 is identified as a potential biomarker for non-small cell lung cancer by integration of the cancer cell secretome and tissue transcriptome. *Int J Cancer*. 2011;128(10):2364-2372. doi:10.1002/ijc.25568
43. Alnoumas L, van den Driest L, Apczynski Z, et al. Evaluation of the role of KPNA2 mutations in breast cancer prognosis using bioinformatics datasets. *BMC Cancer*. 2022;22(1):874. doi:10.1186/s12885-022-09969-4
44. Liao WC, Lin TJ, Liu YC, et al. Nuclear accumulation of KPNA2 impacts radioresistance through positive regulation of the PLSCR1-STAT1 loop in lung adenocarcinoma. *Cancer Sci*. 2022;113(1):205-220. doi:10.1111/cas.15197
45. Mertins P, Mani DR, Ruggles KV, et al. Proteogenomics connects somatic mutations to signalling in breast cancer. *Nature*. 2016;534(7605):55-62. doi:10.1038/nature18003
46. Krug K, Jaehnig EJ, Satpathy S, et al. Proteogenomic landscape of breast cancer tumorigenesis and targeted therapy. *Cell*. 2020;183(5):1436-1456.e31. doi:10.1016/j.cell.2020.10.036
47. Vasaikar S, Huang C, Wang X, et al. Proteogenomic analysis of human colon cancer reveals new therapeutic opportunities. *Cell*. 2019;177(4):1035-1049.e19. doi:10.1016/j.cell.2019.03.030
48. Liu XS, Zhou LM, Yuan LL, et al. NPM1 is a prognostic biomarker involved in immune infiltration of lung adenocarcinoma and associated with m6A modification and glycolysis. *Front Immunol*. 2021;12:724741. doi:10.3389/fimmu.2021.724741

49. Sun C, Gao Y, Yang L, et al. NPM1A in plasma is a potential prognostic biomarker in acute myeloid leukemia. *Open Life Sci.* 2018;13(1):236-241. doi:[10.1515/biol-2018-0028](https://doi.org/10.1515/biol-2018-0028)
50. Peng HH, Ko HH, Chi NC, et al. Upregulated NPM1 is an independent biomarker to predict progression and prognosis of oral squamous cell carcinomas in Taiwan. *Head Neck.* 2020;42(1):5-13. doi:[10.1002/hed.25971](https://doi.org/10.1002/hed.25971)
51. Karimi Dermani F, Gholamzadeh Khoei S, Afshar S, Amini R. The potential role of nucleophosmin (NPM1) in the development of cancer. *J Cell Physiol.* 2021;236(11):7832-7852. doi:[10.1002/jcp.30406](https://doi.org/10.1002/jcp.30406)
52. Zheng S, Li X, Deng T, et al. KPNA2 promotes renal cell carcinoma proliferation and metastasis via NPM. *J Cell Mol Med.* 2021;25(19):9255-9267. doi:[10.1111/jcmm.16846](https://doi.org/10.1111/jcmm.16846)
53. Griss J, Perez-Riverol Y, Lewis S, et al. Recognizing millions of consistently unidentified spectra across hundreds of shotgun proteomics datasets. *Nat Methods.* 2016;13(8):651-656. doi:[10.1038/nmeth.3902](https://doi.org/10.1038/nmeth.3902)

## SUPPORTING INFORMATION

Additional supporting information can be found online in the Supporting Information section at the end of this article.

**How to cite this article:** Huang J-X, Wang C-I, Kuo C-Y, et al. Oxidative stress mediates nucleocytoplasmic shuttling of KPNA2 via AKT1-CDK1 axis-regulated S62 phosphorylation. *FASEB BioAdvances.* 2024;6:276-288. doi:[10.1096/fba.2024-00078](https://doi.org/10.1096/fba.2024-00078)